Available online at www.sciencedirect.com
ScienceDirect
Journal of Magnetism and Magnetic Materials 312 (2007) 390–399
www.elsevier.com/locate/jmmm

Ferromagnetic cobalt nanocrystals achieved by soft annealing approach—From individual behavior to mesoscopic organized properties

C. Petit[a], Z.L. Wang[b], M.P. Pileni[a,*]

[a]Laboratoire des Matériaux Mésoscopiques et Nanométriques, UMR CNRS 7070, Université P. et M. Curie, 4 place Jussieu 75251 Paris, Cedex, France
[b]School of Materials Science and Engineering, Georgia Institute of Technology, Atlanta, GA 30332-0245, USA

Received 29 July 2006; received in revised form 13 October 2006
Available online 27 November 2006

Abstract

By gentle annealing, 7 nm cobalt nanoparticles synthesized by soft chemistry, are transformed to hard magnetic hexagonal close packed (HCP) cobalt nanocrystals without changing the size, size distribution and passivating layer. This method permits to recover the nanocrystals isolated in solution after the annealing process and then to study the magnetic properties of the HCP cobalt nanocrystals at isolated status or in a self-organized film. Monolayer self-assembly of the HCP cobalt nanocrystals is obtained, and due to the dipolar interaction, ferromagnetic behavior close to room temperature has been observed. The magnetic properties differ significantly due to the influence of the substrate on the annealing process. This different approach of the annealing process of nanocrystals is compared to the classical approach of annealing in which the nanocrystals are first deposited on a substrate and then annealed.

Keywords: Nanocrystals; Magnetism; Self-organization

1. Introduction

Organization of small, nanoscale ferromagnetic particles opens an important field of technologies through the controlled fabrication of mesoscopic materials with unique magnetic properties [1]. Technologically, these ferromagnetic nanoparticles are potential candidates for magnetic data storage. The idea is that each ferromagnetic particle may correspond to one bit of data [2,3]. Thin granular films of ferromagnetic particles formed by sputter deposition are already the basis of conventional magnetic storage media. However, devices based on ferromagnetic nanocrystals are limited by the thermal fluctuations of the magnetization of small size particles, because ferromagnetic nanocrystals become superparamagnetic at room temperature [4]. On the other hand, information can be perturbed between adjacent nanocrystals in an array, the dipolar magnetic interactions are also an important limiting factor for their use in magnetic storage. Thus, a detailed understanding on the magnetic properties of assemblies of nanocrystals is essential to the development of future magnetic recording technology.

One of the major problems is to overcome the superparamagnetism of nanocrystals especially when their sizes are small. Whatever the synthesis route is taken, post-synthesis processing is required to obtain ferromagnetic particles that are magnetically stable at room temperature. Experimentally, it is possible to obtain soft ferromagnetic or superparamagnetic nanocrystals and then transform them to harder magnetic phase. This has been illustrated for transforming face-centered cubic (FCC) structured FePt to face-centered tetragonal (FCT) structured at 560 °C [5–7]. Similar thermal treatments are needed in CoPt nanoalloys [8,9]. The ferromagnetic behavior is reached at room temperature; however, the annealing temperature is so high that often, drastic coalescence takes place and the organization is lost. By using the organometallic route, it has been possible to make cobalt nanocrystals with high crystallinity [11]. Their structure

*Corresponding author. Tel.: +33 1 44 27 26 96; fax: +33 1 44 27 25 15.
E-mail address: pileni@sri.jussieu.fr (M.P. Pileni).

0304-8853/$ - see front matter © 2006 Elsevier B.V. All rights reserved.
doi:10.1016/j.jmmm.2006.10.1096

was either FCC, a mixture of FCC–hexagonal close packed (HCP) or the ε phase [10–13]. By annealing for several hours at 300 °C and 500 °C, ε-Co nanocrystals produced via organo-metallic process transit to the HCP and FCC phase, respectively [12]. Again, this long annealing partially destroys the nanocrystal organization and then changes the interparticle distances, which is a key parameter for controlling of the dipolar interaction. This is due to the desorption or burning of the coating agent. As a consequence, it is impossible to recover the isolated nanocrystals and then study the behavior of the individually annealed nanocrystals. Furthermore, the system is not ferromagnetic at or close to room temperature. In this article, we describe in detail the phase transformation of cobalt nanocrystals obtained by wet chemical route from a low-crystallinity state to the HCP state while keeping their identity and ability to self-organize. Hence, 2D mesostructures made of HCP cobalt nanocrystals are obtained. Their magnetic properties are studied and compared to that observed after soft annealing of the mesostructure made using the as-synthesized nanocrystals deposited on a highly oriented pyrolitic graphite (HOPG) substrates. Fast and moderate annealing yields to organization of magnetic nanocrystals with a blocking temperature close to room temperature.

2. Apparatus

2.1. Transmission electron microscopy (TEM)

A JEOL (100 kV) model JEM 100CX II is used for the low-resolution pictures and a Phillips CM20 with a CCD camera for the high-resolution TEM (HRTEM).

2.2. Magnetic properties

The magnetic measurements are made with a commercial SQUID magnetometer (Cryogenic S600) from the SPEC (CEA-Saclay, France).

3. Synthesis and characterization of the cobalt nanocrystals

Cobalt metallic nanocrystals are produced via colloidal assemblies, and they are characterized by EXAFS spectroscopy [14] and X-rays diffraction [15]. No cobalt atoms linking to oxygen atoms have been observed in the material. However, due to the nature of the reducing agent, boron may still be present in the cobalt matrix [14]. The nanocrystals, passivated by lauric acid ($CH_3(CH_2)_{10}COOH$), are dispersed in hexane forming an optically transparent solution of concentration 5×10^{-7} M. The size distribution of the 7 nm cobalt nanocrystals is rather large ($\sigma = 17\%$). To self-assemble them, the sample is prepared as follows: a substrate such as HOPG (for SQUID experiment) or a TEM grid covered by amorphous carbon (for characterization) is deposited in the bottom of a cell containing 200 μl of 5×10^{-7} M cobalt nanocrystal solution. The solution evaporates slowly, yielding to the formation of the self-organized monolayer [10,15–17].

4. Magnetic measurements and analysis

The magnetic properties of the solution containing the nanocrystals or of the mesotructure are study by SQUID measurement. The susceptibility behavior is measured by a zero field cooled (ZFC)/field cooled (FC) experiment. The ZFC/FC experiment allows us to quantitatively study the annealing effect on supported and isolated nanocrystals. In the ZFC, the sample is cooled down to 3 K without applying field starting from a temperature where all of the particles are in the superparamagnetic state. Afterwards, a 75 Oe field is applied and the magnetization as a function of the increasing temperature is measured. In the case of an ideal system of perfectly monodisperse particles, the magnetization measured in the ZFC curve drops upon cooling from the maximum to zero in a few degrees. The temperature T_B at which the susceptibility peak occurs represents the particle blocking temperature, which is related to the particle magnetic anisotropy energy (MAE) K_aV by the relation $K_aV = k_BT_B\,ln(1/f\tau_0) \approx 28\,k_BT_B$, where V is the particle volume, K_a is the MAE per unit volume and $\tau_0 \approx 10^{-9}$–10^{-11} s [18]. The width of this transition (i.e., the distribution of MAE) becomes larger with increasing the size dispersion of the particles: For nanocrystals having large size distribution, the volume V has to be replaced by an effective volume V_{eff} proportional to the average volume, $V_{eff} = \langle V^2\rangle/\langle V\rangle$ [19]. This gives an average value of the MAE.

The hysteresis curves are recorded at 3 K far away from the superparamagnetic state and the field direction is kept parallel to the plane of self-assembled layer.

5. Results and discussion

5.1. Annealing process

At the end of the synthesis, cobalt nanocrystals coated with lauric acid are dispersed in hexane. Two annealing procedures are used:

A The solvent of the colloidal solution is evaporated in a glove box in nitrogen. The beaker with the remaining black film made of uncoalesced cobalt nanocrystal is then annealed at 275 °C for 15 min in nitrogen. After fast cooling at room temperature, hexane is added to the beaker and the solution is subjected to sonication. A small fraction of the films remains in the bottom of the beaker but most of the material is dispersed, forming a stable solution. This method is limited in the annealing temperature up to 300 °C and the annealing time of less than 30 min. Higher than these values, it is not possible to disperse the nanocrystals again in hexane.

B Colloidal solution is deposited on a substrate (HOPG or copper TEM grid coated by amorphous carbon, see

above). As-synthesized cobalt nanocrystals self-organize in 2D superlattice at the mesoscopic scale. The system is then annealed in nitrogen for 15 min at the desired temperature.

In both methods, the sample is introduced in the oven only when the desired temperature is reached to minimize the annealing time. Then, the sample is fast cooled to room temperature.

5.2. Structural investigation of the annealing effect on supported or not cobalt nanocrystals

The as-synthesized nanocrystals are dispersed in hexane and a droplet solution is deposited on TEM grid. For the as-synthesized nanocrystals, Fig. 1(a) shows nanoparticles locally ordered and having 7 nm and 17% as average diameter and size distribution, respectively. The corresponding selected area electron diffraction (SAED) pattern shows two diffuse rings at ~2 and 1.25 Å, indicating a low degree of crystallinity of the as-synthesized cobalt nanoparticles (Fig. 1(b)). The HRTEM image recorded from the as-synthesized nanoparticles (inset of Fig. 1(a)) shows a poor crystallinity, where the wavy lattice fringes are observed. It should be noticed that in some cases a shell is observed surrounding the nanocrystals (Fig. 1(a)). This shell increases during long exposition to the electron beam in TEM. It is likely that the shell could come from the electron-beam-induced contamination. The shell cannot be due to an oxide layer as no ring at 2.46 Å, in correspondence to the oxide phase, is being observed in the SAED patterns. The observed shell, which presents a very low contrast in TEM, could be also provided from the lauric acid attached at the nanocrystals interface.

The TEM image (Fig. 1(c)) obtained by the deposition of the 275 °C annealed nanocrystals (process A) shows a slight decrease in the nanoparticle ordering, in the average diameter (6.8 nm) and size distribution (15%) (Fig. 2). The difference in size and distribution is explained by the fact that, due to desorption of lauric acid from the nanocrystals interface, the annealing process induces limited nanoparticles precipitation. In fact, after annealing, some nanocrystals remain in the bottom of the vessel and cannot be dispersed in hexane. The lack in passivating agent explains the fact that the nanocrystals ordering decreases with annealed nanocrystals compared to

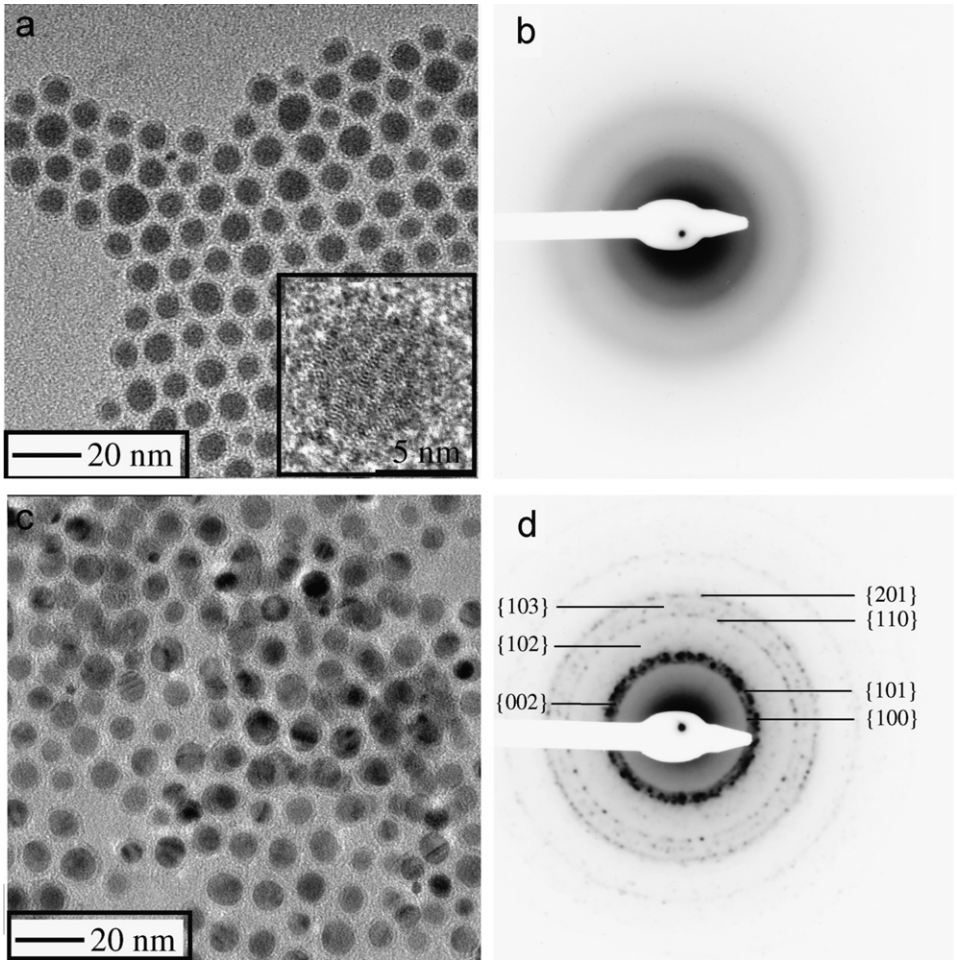

Fig. 1. Structural characterization of cobalt nanocrystals. (a,b) TEM picture and selected area electron diffraction (SAED) of as-synthesized cobalt nanocrystals; (c,d) TEM picture and SAED of cobalt nanocrystals annealed at 275 °C and redispersed in hexane.

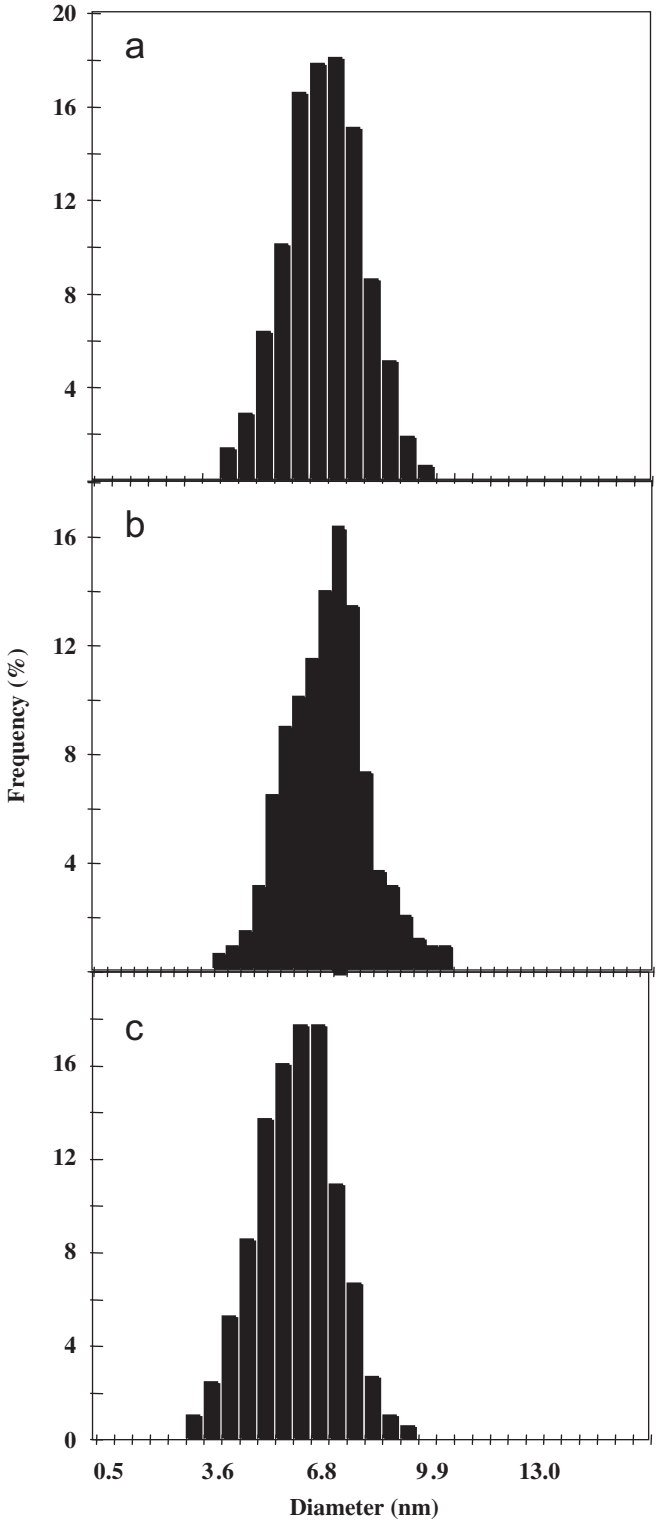

Fig. 2. Size distribution of the: (a) as-synthesized cobalt nanocrystals; (b) HCP cobalt nanocrystals after annealing at 275 °C following procedure A; (c) HCP cobalt nanocrystals after annealing on substrates at 275 °C following procedure B.

as-synthesized one (Fig. 1(a and b)). Distinct from the as-synthesized cobalt (Fig. 1(b)), the electronic diffraction shows spot, forming a pattern of rings at 2.13, 2.02, 1.89, 1.46, 1.24, 1.14 and 1.05 Å (Fig. 1(d)) corresponding to the

Table 1
SAED characterization of the annealed cobalt nanocrystals: (d_{dhkl} in Å) compared to the reference materials

SAED d_{dhkl}	Co_{HCP} line d_{dhkl} spacing, intensity[a]	Co_{FCC} line d_{dhkl} spacing, intensity[b]	CoO line d_{dhkl} spacing, intensity[c]
			2.46 (1 1 1) 75
2.13	2.16 (1 0 0) 27		2.13 (2 0 0) 100
2.02	2.02 (0 0 2) 30	2.05 (1 1 1) 100	
1.89	1.91 (1 0 1) 100		
1.46	1.48 (1 0 2) 2		1.51 (2 2 0) 50
1.25	1.25 (1 1 0) 10	1.25 (2 2 0) 25	1.28 (3 1 1) 20
			1.23 (2 2 2) 15
1.14	1.15 (1 0 3) 10		
1.05	1.04 (2 0 1) 15	1.07 (3 1 1) 30	

[a]Co HCP JCPDS collection code: 5-727.
[b]Co fcc JCPDS collection code: 15-806.
[c]CoO JCPDS collection code: 9-402.

diffraction patterns of cobalt metal in HCP phase: 2.16, 2.03, 1.91, 1.48, 1.25, 1.14 and 1.04 Å (see Table 1). External rings due to the graphite are discernible and no additional ring at 2.46 Å is observed, indicating the absence of cobalt oxide (see Table 1). The intensities and the positions of the peaks exclude the formation of the ε phase Co [20,21] as well as FCC cobalt nanocrystals [21]. The nanocrystals show strong diffraction contrast, which is absent prior to annealing (Fig. 1(a and b)). Such strong diffraction effect clearly confirms the high crystallinity of the nanoparticles. The contrast suggests that some of the particles are composed of multiple grains. In fact, the HRTEM images (Fig. 3(a and b)) show formation of monocrystals with an interlattice distance of $2+/-0.05$ Å, consistent to the 2.02 Å lattice spacing for the (0 0 2) planes and the 1.91 Å spacing for the (1 0 1) planes of HCP cobalt. The particle in Fig. 3(a) is likely to be a single crystal. The particle in Fig. 3(b) is composed of grains that are linked by stacking faults and twins, as suggested by the bending of the lattice fringes across the particle.

From these data, it is concluded that this gentle annealing permits to improve the crystallinity of the nanoparticles obtained by soft chemistry and to keep their ability to be dispersed in a solvent; consequently, to produce 2D monolayer self-assembly or eventually other patterns, in low interaction with the substrate.

Conversely to that described above, in procedure B, the as-synthesized cobalt nanocrystals are first deposited on a substrate forming a 2D monolayer and the supported mesostructure is annealed. This technique has been already used by other group [22–24]. Hence monolayers of cobalt nanocrystals deposited either on HOPG or amorphous carbon (on TEM grid) as substrate are annealed or not at 275 °C. The organization of the monolayers before (Fig. 1(a) and after (Fig. 4(a)) remains the same and no aggregation process takes place. As for process A, the diffraction pattern of the annealed monolayer shows the characteristics patterns of the cobalt in HCP structure

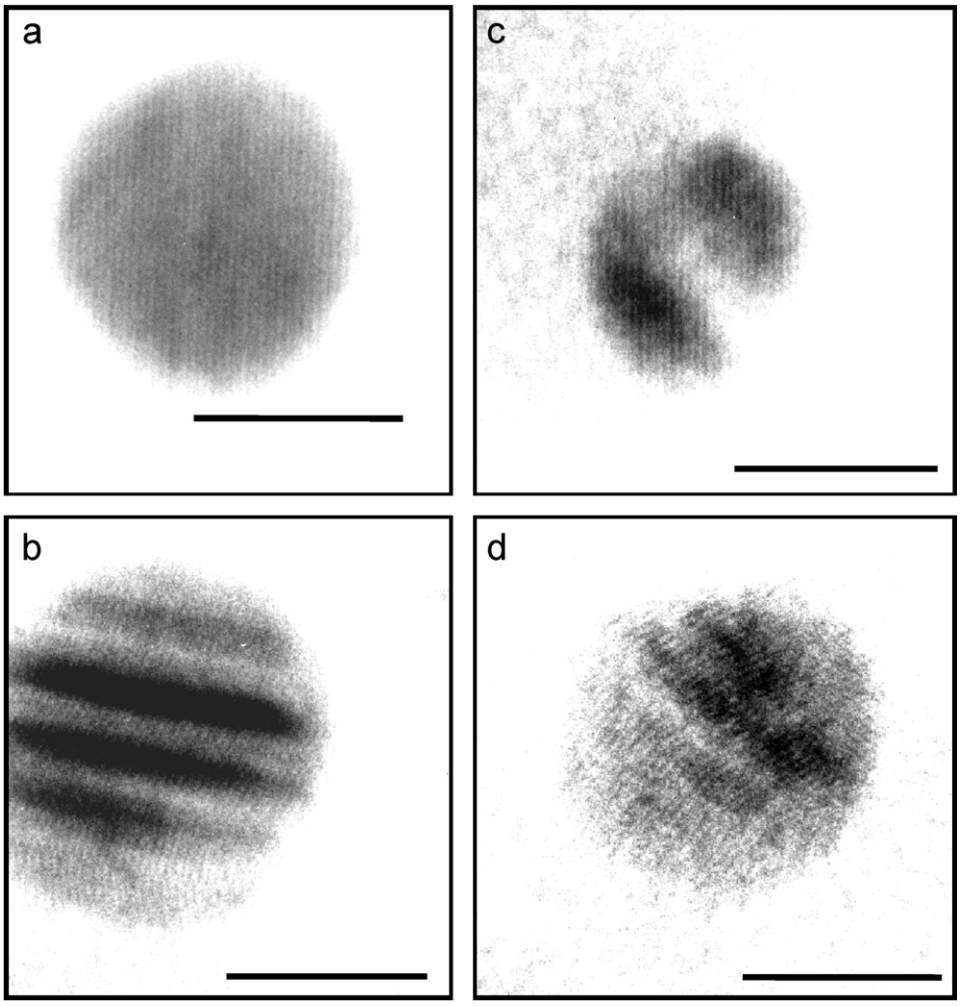

Fig. 3. HRTEM images of cobalt nanocrystals (a,b) annealed at 275 °C following procedure A and redispersed in hexane; (c,d) annealed as 2D monolayers on the TEM grid following procedure B.

(Fig. 4(b)). However, the average size of the nanocrystals before and after annealing decrease from 7 to 6.2 nm whereas their distribution remains unchanged (18% instead of 17%) (Fig. 2). Furthermore, the interparticle distance decreases and then the monolayer compacity increases (Fig. 4(a)). This could be due to vaporization of boron included in the matrix during the reduction of cobalt ions by sodium borohydride ($NaBH_4$). It could not be an excluded artifact due to the annealing of the amorphous carbon on the TEM grid during the annealing process. It could also result from the electron-beam-induced contamination, which may limit the possibility of HRTEM study. HRTEM shows the same kind of structure reported above but with a lower picture quality (Fig. 3c and d). Hence, the substrate could perturb the annealing. As a matter of fact, Nie et al. [23] reported, for cobalt nanocrystals embedded in amorphous carbon and subjected to annealing, the influence of the carbon matrix on the coalescence, the crystallographic structure and magnetic properties of the cobalt nanocrystals [23].

For the 2D monolayer annealed at intermediate temperature (250 °C), as above no change in the nanocrystal assembly is observed (Fig. 4(c)). The electron diffraction pattern shows narrower rings with some spots (Fig. 4(d)). This indicates a lower crystallinity than the monolayer annealed at 275 °C but an increase compared to the as-synthesized nanocrystals. The spots are due to the fact that some nanocrystals have a preferential orientation in reference to the electronic beam. However, the transition is not complete. In the TEM image of the nanocrystals assembly (Fig. 4(b)), some particles appears to be coalesced. This does not seem to be the case (see below the magnetic properties): it is more probably due to the fact that the monolayer are not perfect and few nanoparticles could set on a second layer; in fact, TEM gives the projected image.

The study developed above shows that whatever the procedure used, the crystallinity of cobalt nanoparticles is strongly improved with formation of the HCP monocrystal phase. Furthermore, the self-organization is always maintained under annealing. However, the annealing process A is a very powerful approach because it is easy to keep the versatility in the self-organization of the nanocrystals. This opens a possibility to grow ''supra-crystals'' made of HCP cobalt nanocrystals.

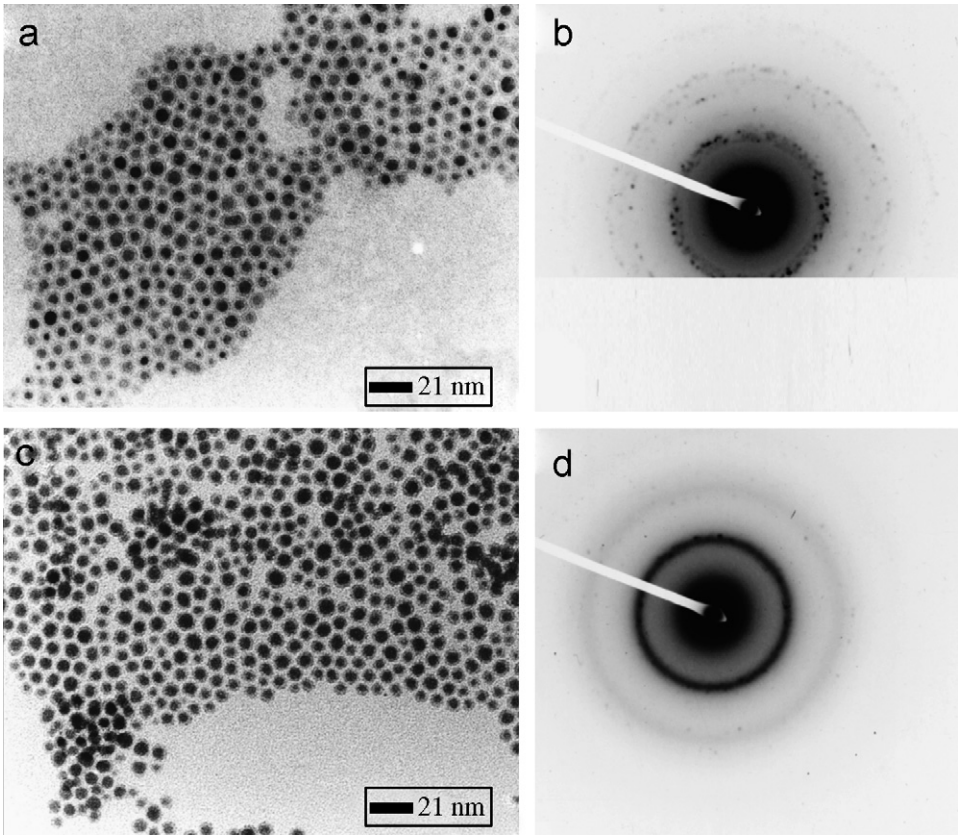

Fig. 4. TEM images (a,c) and SAED patterns (b,d) of cobalt nanoparticles annealed with procedure B; (a,b) deposited on TEM grid and annealed at 275 °C; (c,d) deposited on TEM grid and annealed at 250 °C.

Table 2
Magnetic properties of cobalt nanocrystals depending on their annealing and on the organization

Sample	T_b (K)	M_s (emu/g)	H_c (T)	M_r/M_s
As synthesized Co isolated	65	85 ± 5	0.18	0.35
Co HCP isolated (annealed at 275)	215	145 ± 5	0.13	0.45
Co HCP In 2D monolayer	275	145 ± 5	0.11	0.52
Co as synthesized In 2D monolayer	80	85 ± 5	0.18	0.49
Co as synthesized In 2D monolayer annealed at 275	245	145 ± 5	0.11	0.50

5.3. Comparison of the magnetic properties depending on the annealing process

5.3.1. Magnetic properties of isolated nanocrystals

The magnetic properties of as-synthesized and the 275 °C annealed nanocrystals (process A) dispersed in hexane (i.e., without interactions) are compared. The ZFC curve (Fig. 5 and Table 2) shows a blocking temperature of the as-synthesized nanocrystals (7 nm, 17% as average diameter and size distribution) being 65 K, while that of the annealed nanocrystals (6.8 nm as average diameter, 15% in size distribution) is 215 K (Fig. 5(a)). The relative width distribution of the MAE, K_a, decreases for 275 °C annealed nanocrystals compared to the as-synthesized one (inset of Fig. 5(a)). This indicates a strong decrease in the MAE dispersion due to the formation of cobalt HCP monocrystals. In fact, a slight change in the size distribution (from 17 to 15%) cannot be taken into account (Fig. 2). From the blocking temperature, the MAE, K_a, of the isolated nanocrystals evolves from 1.5×10^6 to 4.5×10^6 erg/cm^3 by annealing. The first value is consistent with the previous data obtained for as-synthesized cobalt nanocrystals [8,13], and the second one is closed to the bulk values of the cobalt in HCP structure (4.5×10^6 erg/cm^3) [25].

At 3 K, the hysteresis loop of the as-synthesized cobalt nanocrystals does not reach saturation magnetization at 2.5 T, which is estimated to be 85 ± 5 emu/g (from the extrapolation of M vs. $1/H$) with 0.18 T as coercivity (Fig. 6(a) dotted lines). After annealing at 275 °C, the saturation magnetization, reached at 2 T, markedly

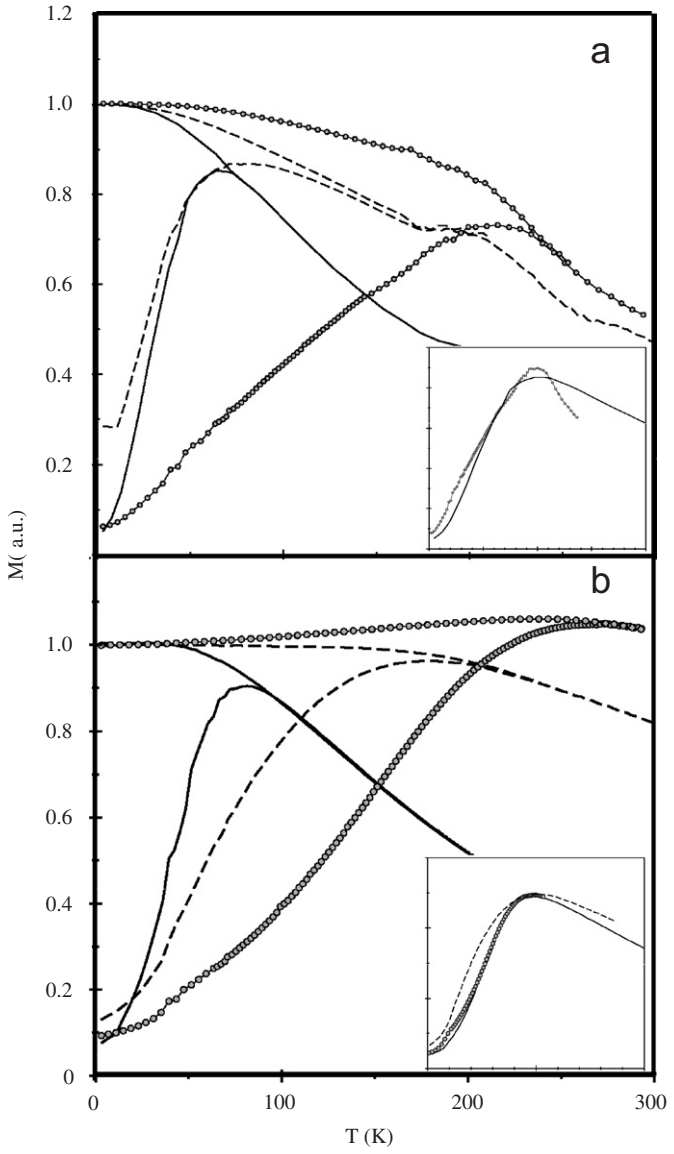

Fig. 5. Zero field cooled/field cooled curves of cobalt nanoparticles: (a) dispersed in hexane: as-synthesized (solid line), annealed at 250 °C with procedure A (dotted line), annealed at 275 °C with procedure B (open circle); (b) deposited on HOPG substrate: as-synthesized (solid line), annealed at 250 °C with procedure A (dotted line), annealed at 275 °C with procedure A (open circle).

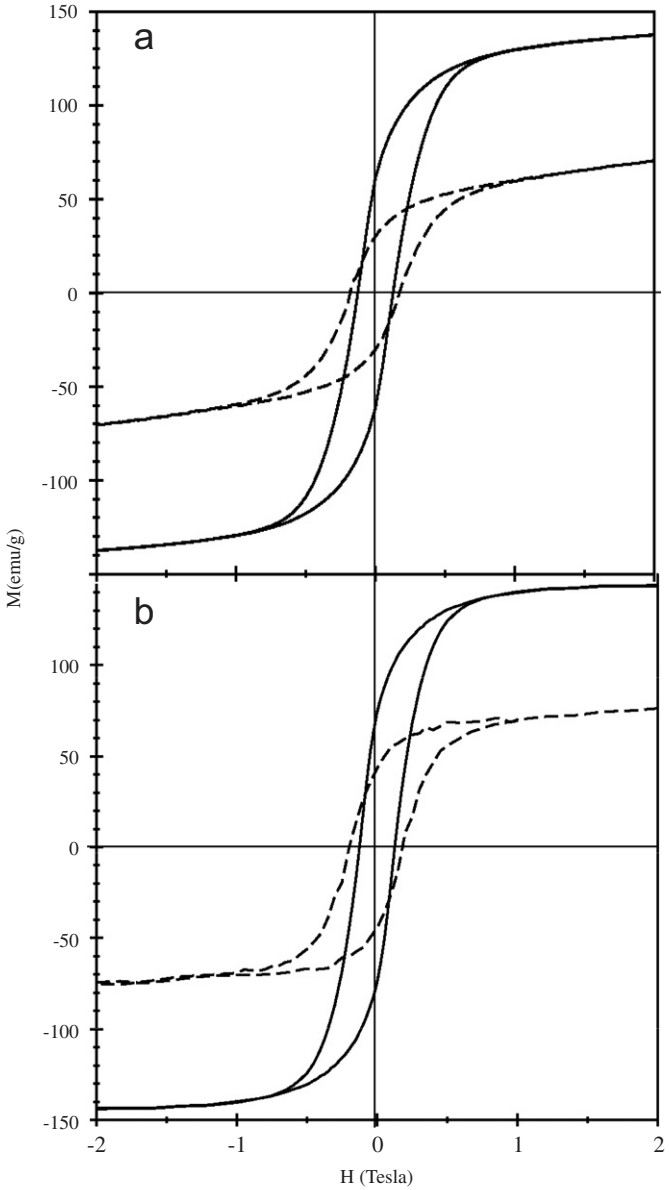

Fig. 6. Comparison of the hysteresis loop at 3 K of the as-synthesized (dotted line) and annealed at 275 °C with procedure A (solid line): (a):dispersed in hexane solution (i.e., isolated without interaction); (b) self-assembled on HOPG substrates in 2D monolayers.

increases to 145 ± 5 emu/g (Fig. 6(a), solid line). Furthermore, an increase in the reduced remanence to 0.45 and a decrease in the coercivity to 0.13 T are observed (Table 2). The change in the reduced remanence is easily explained by the change in the crystalline structure of nanocrystals. In fact, cobalt nanocrystal in the HCP structure presents a uniaxial anisotropy with a calculated reduced remanence value of 0.50 [26]. The slight difference between the experimental and calculated value is attributed to surface spin canting effect. More surprising is the increase in the saturation magnetization from 85 to 145 emu/g. This is explained as follows: the as-synthesized cobalt nanocrystal is made of small crystalline domains separated by amorphous material of cobalt and/or cobalt/boron (inset of Fig. 1(a)). Each crystalline domain is characterized by its own magnetic moment oriented randomly. The total magnetic moment of the nanoparticle is the sum of these magnetic domains coupled by dipolar interactions. As a result, a low value of M_s is obtained. By annealing, monocrystals are formed and these nanodomains disappear (Fig. 3(a and b)). A monocrystalline phase, characterized by a uniaxial moment, is produced. The saturation magnetization (145 emu/g) is then close to that of the bulk phase (162 emu/g). Again, the slight difference between these two values is attributed to the surface effect and the adsorbed coating agent. The decrease in coercivity after annealing is due to a decrease in the surface defect during the process. In fact, this defect

could act as a trap preventing the flip of the magnetic moment.

Hence, cobalt nanocrystals in their HCP structure are a harder magnetic material compared to the as-synthesized cobalt nanocrystals. This magnetic phase transition is demonstrated by considering the magnetic properties of cobalt nanocrystals annealed at lower temperature, 250 °C. The ZFC/FC curve shows two broad bands (Fig. 5(a), dotted line). The first one centered at 85 K, corresponding to the as-synthesized nanocrystals, and the second one is centered at 190 K, corresponding to nanocrystals partially transformed into the HCP phase. Hence, a transition is really obtained from a soft magnetic cobalt nanocrystal to a hard magnetic cobalt nanocrystal.

5.3.2. Effect of the annealing process on the collective magnetic properties

In previous articles, we have demonstrated that as a result of the dipolar interaction, the magnetic properties of an assembly of as-synthesized nanocrystals deposited on a substrate differ from those obtained with the same nanocrystals dispersed in a solvent (without interactions between nanocrystals) [14,15,27]. As expected, similar behavior is observed with both as-synthesized and annealed nanocrystals (process A). In fact with as-synthesized cobalt nanocrystals, the blocking temperature (Fig. 5(b), solid line) and the reduced remanence (Fig. 6(b), dotted line) increase from 65 to 80 K and 0.35–0.49, respectively, when nanocrystals are isolated and deposited on HOPG (Table 2). For the 275 °C annealed nanocrystals, the blocking temperature increases from 215 to 275 K when the HCP nanocrystals are deposited on a substrate. As expected, the hysteresis loop is squarer and the reduced remanence increases from 0.45 to 0.52 with a slight decrease in coercivity (from 0.13 to 0.11 T). These changes in the magnetic properties are attributed to dipolar interaction between nanocrystals [28]. Inset of Fig. 5(b) shows that the normalized ZFC curve for 2D monolayer of the as-synthesized and annealed nanocrystals completely superimposed. This markedly differs from the ZFC curve of the same nanocrystals dispersed in solution (inset of Fig. 5(a)). This is explained by the fact that the dipolar interactions do not markedly differ after annealing. This is estimated by taking into account the coupling dipolar interaction constant, defined as the ratio of the dipolar to the anisotropy energies. The coupling constant is deduced from Stoner–Wolfarth model as $\alpha_d = (\pi M_s^2/12\,\mathrm{K}) \times (D/d)^3$, where D and d are the average diameter and the interparticle distance, respectively [27,28]. The annealing process induces simultaneously an increase in the saturation magnetization and in the anisotropy constant. The increase in the saturation magnetization is compensated by that of the anisotropy constant and keeps the coupling constant unchanged. In fact, it is 0.040 and 0.039 for the as-synthesized and annealed nanocrystals, respectively. This difference is not significant and indicates that the dipolar interaction between nanocrystals remains unchanged before and after annealing. This explains the invariant of the distribution of the MAE when the nanocrystals are deposited in 2D monolayers, as the dipolar interactions average over the individual behavior. As demonstrated previously [28], the local ordering in the monolayer does not play a role in the collective magnetic properties. Hence the loss of organization observed for the annealed nanocrystals does not modify the interaction.

For the monolayers made with nanocrystals annealed at intermediate temperature, 250 °C, there is only one broad band centered at 190 K (Fig. 5(b), dotted line). It is in fact an average of the two bands previously observed for the isolated nanocrystals (Fig. 5(a), dotted line). This is due to the long-range dipolar interaction. As a matter of fact, the inset of Fig. 5(b) shows the distribution of MAE, which is larger than that of the monolayer made of the as-synthesized or HCP cobalt nanocrystals.

One question arises: Does the procedure used to obtain a monolayer of HCP cobalt nanocrystals change their magnetic properties?

To answer the question, we consider the sample annealed at 275 °C according to procedure B and we compare their magnetic properties to the previous one. The blocking temperature is 80 K for the 2D monolayers made of as-synthesized nanoparticles. For the 275 °C annealed monolayer, the blocking temperature increases to 245 K (Fig. 7(a) and Table 2). Comparing to the original 2D monolayers, the width of the MAE distribution remains unchanged (inset of Fig. 7(a)). This indicates an absence of significant coalescence and confirms the TEM investigation.

Let us compare the magnetic behavior of the 2D monolayer made of the 275 °C annealed nanocrystals deposited on the HOPG substrates with that of the 275 °C annealed monolayer. For the hysteresis loop, the change in the magnetic behavior is not very important (Fig. 7(b) and Table 2). It appears a little bit squarer for the monolayer made with Co HCP without changing the magnetization at saturation. There is a slight increase in the reduced remanence (from 0.50 to 0.52) and unchanged coercivity. In fact, the evolution of the magnetic properties between the monolayers described above appears to be dominated by the change in the size distribution and size of the nanocrystals depending on the annealing process. This is clear from the evolution of T_B: it is 275 K for the monolayers made of annealed nanocrystals and 245 K for the annealed monolayers. In fact the size varies from 6.8 to 6.2 nm in the first case, and the polydispersity increases from 15% to 18% in the second case (Fig. 2). This induces a slight decrease in the coupling constant (see above) from $\alpha_d = 0.039$ to 0.036. Hence, as observed experimentally, a higher T_B and squarer hysteresis loop is expected for the monolayer made of the 275 °C annealed cobalt nanocrystals. As reported by Nie et al. [23], we cannot also exclude the effect of the amorphous carbon film on TEM grid during annealing. In fact, the magnetic efficiency of the Co nanocrystals could be degraded due to a mixture of Co and

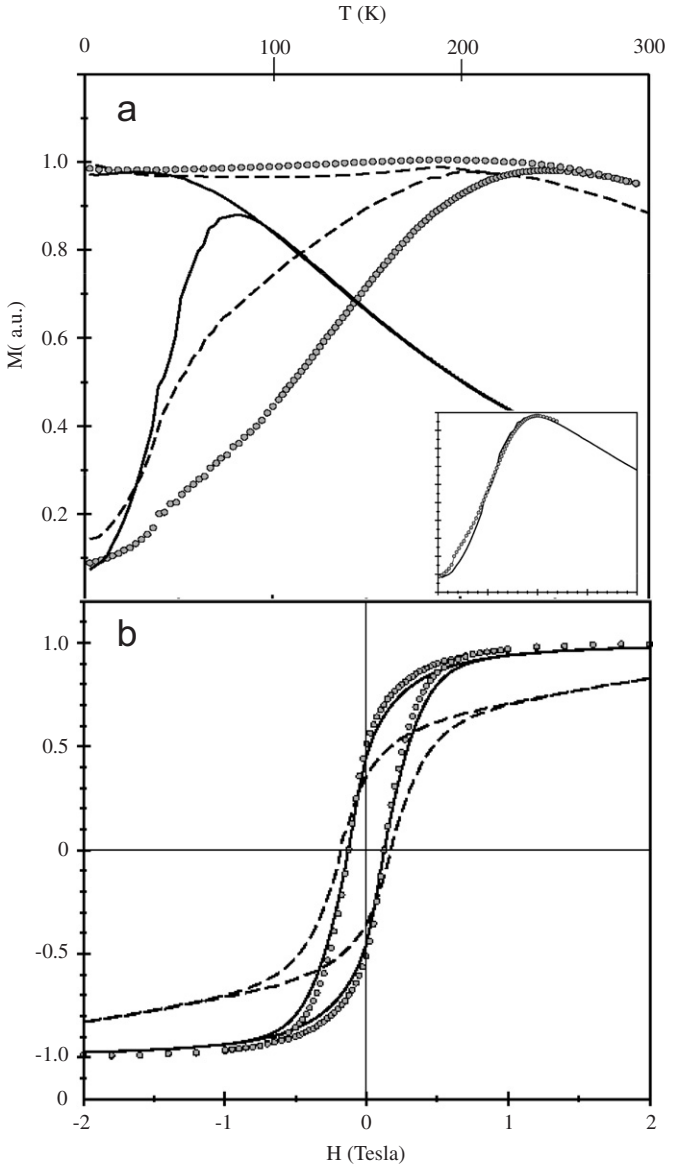

Fig. 7. Magnetic characterization of 2D mesostructures annealed with procedure B (a) zero field cooled/field cooled curves of the 2D monolayers: the as-synthesized (solid lines), annealed at 250 °C (dotted lines), annealed at 275 °C (open circles). (b) Comparison of the hysteresis loop at 3 K of the as-synthesized (dotted line), 2D monolayers annealed at 275 °C (solid lines) and 2D monolayers made of cobalt nanocrystals annealed at 275 °C with procedure A.

carbon at the boundary. This effect could also explain the lower magnetic efficiency of the nanocrystals annealed on a substrate when compared to that annealed following procedure A.

For monolayer annealed at intermediate annealing temperature, 250 °C, the ZFC curves of the annealed monolayer (Fig. 7(a), dotted line) show a broad band centered at 200 K with a shoulder at 80 K. This is similar to what is observed for isolated nanocrystals (Fig. 5(a)). However, the intensity of the two bands is in contrast, as the band at 80 K is only a shoulder. As mentioned above, this is the result of long-range dipolar interaction. The interactions are averaged over the substrates whatever the status of crystallinity of the particles is. As a result, the two bands fuse into one broader band at an intermediate value. This confirms the importance of the dipolar interaction and the effect of annealing on the magnetic signature by ZFC/FC of the monolayers made of nanocrystals.

Hence, both methods of annealing yield similar results; however, the procedure permits to redisperse the nanocrystals, then to get a higher homogeneity in size of the HCP cobalt nanocrystals and then to get a better magnetic behavior. From these data, it is concluded that a gentle annealing induces a transition between poorly crystallized phase to HCP cobalt nanocrystals. This is obtained either for isolated nanocrystals or for supported nanocrystals. These results are consistent with that reported by Wang et al. [29,30] on the annealing of metallic nanocrystals with similar size. Sun et al. [22] reported such a change for supported cobalt nanocrystals from a well-crystallized ε phase to HCP phase for 9 nm cobalt nanoparticles annealed at 570 K. However, the method presented in the current article allows to disperse again the HCP cobalt nanocrystals in solution, and then to study the magnetic properties of the isolated nanocrystals prior to examining their collective properties of the annealed mesostructure and that of mesostructure made using the annealed nanocrystals.

6. Conclusion

Seven nanometer cobalt nanoparticles are synthesized by soft chemistry. They can be organized into 2D monolayers. Due to the collective dipolar interaction and the unique structural effect, drastically improved magnetic properties have been observed. But the limitation is that the ferromagnetism is observed only at low temperature (below 80 K). In this article, we demonstrate that a gentle annealing at 275 °C for 15 min induces a structural transition of the poorly crystallized nanoparticles to monocrystalline HCP cobalt nanocrystals neither coalescence nor changing in size distribution. Due to a strong improvement in magnetization at saturation, from 85 to 145 emu/g and the magnetic anisotropic energy, the ferromagnetic domains of using the nanocrystals is extended toward room temperature while the strength of dipolar interaction is preserved. Mesostructures made of HCP cobalt nanocrystals are obtained and their magnetic properties have been studied and compared to those of the isolated HCP nanocrystals.

References

[1] X. Batlle, A. Labarta, J. Phys. D 35 (2002) R15.
[2] S.A.M. Tofail, I.Z. Rahman, M.A. Rahman, Appl. Organomet. Chem. 15 (2001) 373.
[3] D.N. Lambeth, E.M.T. Velu, G.H. Bellesis, L.L. Lee, D.E. Laughlin, J. Appl. Phys. 79 (1996) 4496.

[4] D.D. Aschwalom, S. Von Molnar, Physical properties of nanomater scale magnets, in: G.L. Timp (Ed.), Edited-Book Title: Nanotechnology, Springer, New York, 1998.
[5] S. Sun, C.B. Murray, D. Weller, L. Folks, A. Moser, Science 287 (2000) 1989.
[6] B. Stahl, et al., Adv. Mater. 14 (2002) 24.
[7] M. Chen, D.E. Nikles, J. Appl. Phys. 91 (2002) 8477.
[8] C. Petit, S. Rusponi, H. Brune, J. Appl. Phys. 95 (2004) 4251.
[9] M. Chen, D.E. Nikles, J. Appl. Phys. 91 (2002) 8477.
[10] Z.L. Wang, Z.R. Dai, S. Sun, Adv. Mater. 12 (2000) 1944.
[11] J. Park, N-J. Kang, Y-W. Jun, S.J. Oh, H-C. Ri, J. Cheon, Chem. Phys. Chem. 6 (2002) 543.
[12] V.F. Puntes, P. Gorostiza, D.M. Aruguete, N.G. Bastus, A.P. Alivisatos, Nat. Mater. 3 (2004) 263.
[13] O. Margeat., C. Amiens, B. Chaudret, P. Lecante, R.E. Benfield, Chem. Mater. 17 (2005) 107.
[14] J. Legrand, C. Petit, D. Bazin, M.P. Pileni, Appl. Surf. Sci. 164 (2000) 186.
[15] C. Petit, A. Taleb, M.P. Pileni, J. Phys. Chem. B 103 (1999) 1805.
[16] Z.L. Wang, Z.R. Dai, S. Sun, Adv. Mater. 12 (2000) 1944.
[17] L. Motte, F. Billoudet, M.P. Pileni, J. Phys. Chem. 99 (1995) 16425.
[18] E. Tronc, Il Nuovo Cimento 18 (D) (1996) 163.
[19] J.L. Dormann, F. D'Orazio, F. Lucari, E. Tronc, P. Prené, J.P. Lolivet, D. Fiorani, R. Cherkaoui, M. Noguès, Phys. Rev. B 53 (1996) 14291.
[20] Y. Bao, M. Beerman, A.B. Pakhomov, K.M. Krishnan, J. Phys. Chem. B 109 (2005) 7220.
[21] V.F. puntes, D. Zanchet, C.K. Erdammez, A.P. Alivisatos, J. Am. Chem. Soc 142 (2002) 12874.
[22] S. Sun, C.B. Murray, J. Appl. Phys. 85 (1999) 4235.
[23] X. Nie, J.C. Jiang, E.I. Meletis, L.D. Tung, L. Spinu, J. Appl. Phys. 93 (2003) 4750.
[24] V. Dureuil, C. Ricolleau, M. Gandais, C. Grisis, J.P. Lacharme, A. Naudon, J. Crystal Growth 233 (2001) 737.
[25] F. Luis, J.M. Torres, L.M. Garcia, J. Bartolomé, J. Stankiewicz, F. Petroff, F. Fettar, J.L. Maurice, A. Vaurés, Phys. Rev. B 65 (2002) 094409.
[26] R.M. Bozorth, Ferromagnetism, vol. XVII, IEEE Press, Piscataway, NJ, 1978.
[27] V. Russier, C. Petit, J. Legrand, M.P. Pileni, Phys. Rev. B 62 (2000) 3910.
[28] V. Russier, J. Appl. Phys. 89 (2001) 1287.
[29] Z.L. Wang, J. Phys. Chem. B 104 (2000) 1153.
[30] Z.L. Wang, J.S. Yin, Mater. Sci. Eng. Struct. 286 (2000) 39.